Journal of Catalysis 281 (2011) 30–39

Contents lists available at ScienceDirect

Journal of Catalysis

journal homepage: www.elsevier.com/locate/jcat

Superior catalytic properties in aerobic oxidation of olefins over Au nanoparticles on pyrrolidone-modified SBA-15

Liang Wang [b], Hong Wang [c], Prokop Hapala [d], Longfeng Zhu [b], Limin Ren [b], Xiangju Meng [a], James P. Lewis [c], Feng-Shou Xiao [a,*]

[a] Key Lab of Applied Chemistry of Zhejiang Province, Department of Chemistry, Zhejiang University (XiXi Campus), Hangzhou 310028, China
[b] State Key Laboratory of Inorganic Synthesis and Preparative Chemistry, Jilin University, Changchun 130012, China
[c] Department of Physics, West Virginia University, Morgantown, WV 26506-6315, USA
[d] Institute of Physics, Academy of Sciences of the Czech Republic, Cukrovarnická 10, 1862 53 Prague, Czech Republic

ARTICLE INFO

Article history:
Received 18 February 2011
Revised 30 March 2011
Accepted 31 March 2011
Available online 10 May 2011

Keywords:
Au nanoparticles
Pyrrolidone
Cyclohexene and styrene oxidation by molecular oxygen

ABSTRACT

We report on our systematic investigation of Au nanoparticles highly dispersed in the mesopores of (s)-(−)-2-pyrrolidinone-5-carboxylic acid (Py)-modified SBA-15 (Au/SBA-15-Py) by using a series of modern techniques. ^{13}C NMR and IR spectroscopies indicate that Py species are successfully grafted on the surface of mesopores in SBA-15; XRD patterns and N_2 adsorption isotherms show that the sample mesostructures are well preserved; TEM images clearly confirm the uniform Au nanoparticles in the mesopores; and XPS suggests an interaction between Au nanoparticles with Py species. Interestingly, Au/SBA-15-Py catalysts always exhibit superior catalytic properties in the oxidation of cyclohexene and styrene by molecular oxygen at atmospheric pressure, compared with the pyrrolidone-free SBA-15 supported Au catalyst (Au/SBA-15-N). This phenomenon is reasonably related to the interaction between Au nanoparticles with Py species, which is consistent with results analyzed from our density-functional theory (DFT) calculations.

1. Introduction

The oxidation of olefins is of great interest and importance in the production of fine chemicals and chemical intermediates [1–4]. Generally, the olefin oxidations are performed by using organic or inorganic oxidants (*tert*-butyl hydroperoxide, TBHP, or $KMnO_4$), which produce a great deal of environmentally undesirable waste [5–8]. Molecular oxygen, which is widely accepted as a green oxidant with obvious advantages including atom economy and low cost, is strongly desirable for a long time. However, the use of molecular oxygen in olefin oxidations is still a challenge [9–11].

It is well known that many metal (Co, Cu and V) compounds are active homogeneous catalysts for olefin oxidations [12–14], but these catalysts have difficulty in separation and regeneration. Heterogeneous catalysts could effectively solve these problems, but their catalytic activities are much lower than those of homogeneous ones. Therefore, heterogenization of homogeneous catalysts on solid supports could combine the advantages of both homogeneous catalysts (high activity) and heterogeneous catalysts (recyclability). For example, Knopsgerrits et al. reported that the complexes of manganese (II) with bipyridine (bpy) entrapped in zeolites are catalytically active and efficiently recyclable catalysts in olefin oxidations [15].

Recently, Au nanoparticles (NPs) are widely used in a series of reactions [16–64]. Particularly, olefin oxidations have attracted much attention since Haruta's pioneer work of direct oxidation of propene over supported Au NPs using molecular oxygen [16]. More recently, Au NPs stabilized in poly (*N*-vinyl-2-pyrrolidone) solution (Au/PVP), a typical homogeneous-like catalyst, shows superior catalytic properties in alcohol oxidations [65,66]. Recently, we have briefly preformed heterogenization of Au/PVP from supporting Au NPs in SBA-15 modified by (s)-(−)-2-pyrrolidinone-5-carboxylic acid (Au/SBA-15-Py), and this catalyst is active in alcohol oxidations [67]. Herein, we have systemically characterized Au/SBA-15-Py catalysts. Furthermore, it is found that Au/SBA-15-Py exhibits excellent catalytic properties in olefin oxidations with molecular oxygen, and we analyze the origin of its high activity from the results of density-functional theory (DFT) calculations.

2. Experimental and computational methodology

2.1. Chemicals and regents

All reagents were of analytical grade and used without further treatment. Nonionic block copolymer surfactant (Pluronic 123, molecular weight of about 5800) was purchased from Sigma–Aldrich Co. (s)-(-)-2-Pyrrolidinone-5-carboxylic acid (Py), cyclohexene epoxide, 2-cyclohexen-1-ol, 2-cyclohexen-1-one, 1, 2-cyclohexanedione, and styrene epoxide were obtained from Alfa Aesar. Co. Styrene,

* Corresponding author. Fax: +86 431 85168624.
E-mail address: fsxiao@mail.jlu.edu.cn (F.-S. Xiao).

0021-9517/$ - see front matter © 2011 Elsevier Inc. All rights reserved.
doi:10.1016/j.jcat.2011.03.029

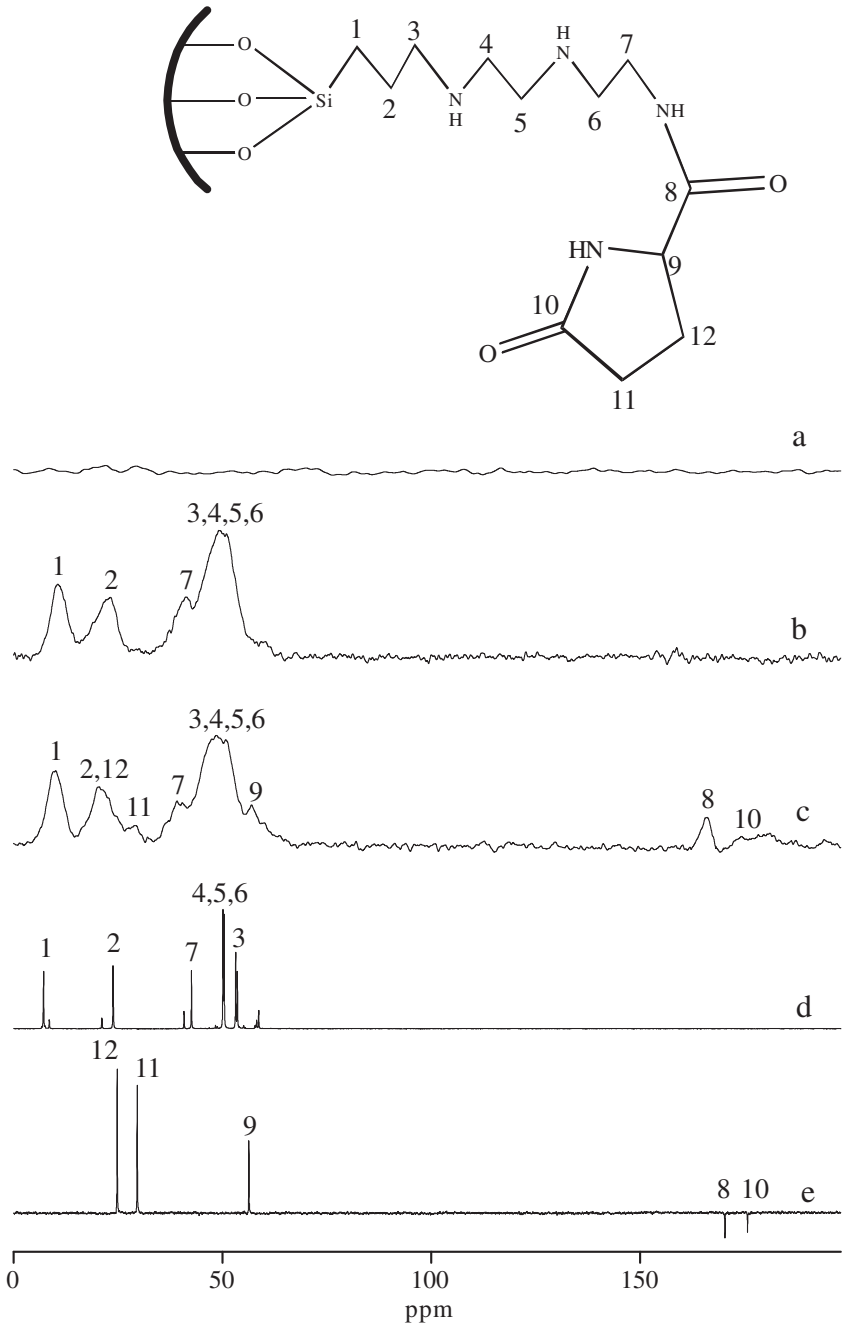

Fig. 1. ^{13}C NMR spectra for solid samples of: (a) SBA-15, (b) SBA-15-N, and (c) Au/SBA-15-Py and liquid samples of (d) DETA and (e) Py.

tetraethyl orthosilicate (TEOS), DMF, cyclohexene, MeCN, and 1,4-dimethylbenzene were bought from Tianjin Chem. Co. HCl, toluene, and ethanol were from Beijing Chem. Co. N-[3-(trimethoxysilyl)-propyl]diethylenetriamine (DETA), 4-dimethylaminopyridine (DMAP), $HAuCl_4{\cdot}4H_2O$, triethylamine (Et_3N), and 1-ethyl-3-(3-dimethyllaminopropyl) carbodiimide hydrochloride (EDC·HCl) were purchased from Shanghai Chem. Co.

2.2. Sample preparation

2.2.1. Preparation of SBA-15

SBA-15 was synthesized according to literature [68]. As a typical run, 0.8 g of copolymer surfactant (P123) was dissolved in 25 mL of water, followed by addition of 3 mL HCl (10 M/L). After stirring at room temperature until complete dissolution of P123 in the aqueous solution, 2.4 mL of TEOS was introduced. After stirring at 313 K for 20 h, the mixture was transferred into an autoclave for condensation at 373 K for 24 h. The as-synthesized samples (SBA-15) were collected by filtration and treated in ethanol containing HCl to remove the surfactants.

2.2.2. Preparation of SBA-15-N

SBA-15-N was prepared from the interaction between SBA-15 with DETA. As a typical run, 1 g of SBA-15 was dried at 393 K under vacuum for 3 h, followed by addition of 50 mL of toluene pretreated by Na and 1 g of DETA. The mixture was refluxed overnight and collected by rotary evaporation, followed by washing with a large amount of ethanol. The sample obtained was designated as SBA-15-N.

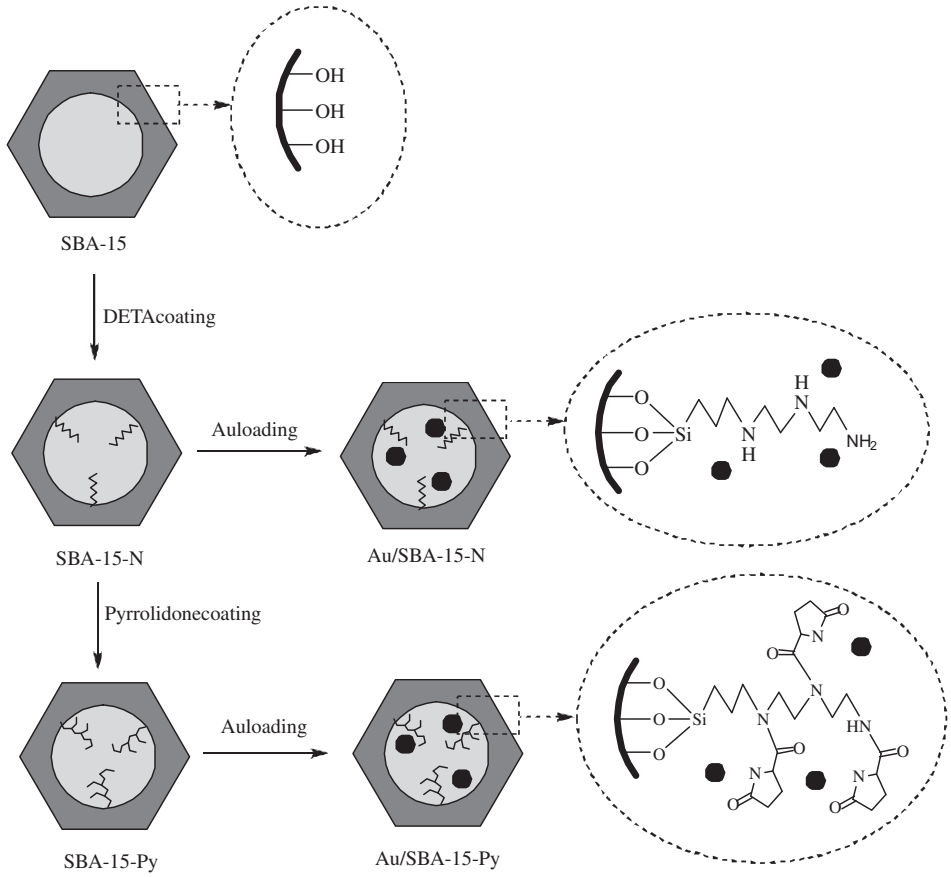

Scheme 1. Procedures for preparation of Au/SBA-15-N and Au/SBA-15-Py catalysts.

2.2.3. Preparation of Au/SBA-15-N

Au/SBA-15-N was prepared by addition of SBA-15-N into $HAuCl_4$ solution, stirring at room temperature for overnight, drying at 373 K under vacuum, reduction by $NaBH_4$ in anhydrous toluene, and washing with a large amount of ethanol and water.

2.2.4. Preparation of SBA-15-Py

To prepare pyrrolidinone-modified SBA-15 (SBA-15-Py), 3.16 g of (s)-(−)-2-Pyrrolidinone-5-carboxylic acid (Py) was dissolved in a mixture of dichloromethane and DMF (molar ratio of dichloromethane/DMF at 10), followed by addition of EDC·HCl and Et_3N (molar ratio of Py/EDC·HCl/Et_3N at 1/1.5/1.5). After stirring at room temperature for 20 min, 1 g of SBA-15-N and a small amount of 4-dimethylaminopyridine (DMAP, 10 mg) were introduced, stirring at room temperature for overnight under anhydrous condition. The sample (SBA-15-Py) was collected by filtration and washing with a large amount of ethanol and water.

2.2.5. Preparation of Au/SBA-15-Py

Au/SBA-15-Py was prepared from mixing SBA-15-Py with $HAuCl_4$ solution for overnight at room temperature, followed by dryness at 373 K under vacuum, reduction by $NaBH_4$ in anhydrous toluene, and washing with a large amount of ethanol and water.

2.3. Sample characterization

Powder X-ray diffraction patterns (XRD) were obtained with a Siemens D5005 diffractometer and Rigaku D/MAX 2550 diffractometer with Cu Kα radiation (λ = 0.1542 nm). Transmission electron microscopy (TEM) experiments were performed on a JEM-3010 electron microscope (JEOL, Japan) with an acceleration voltage of 300 kV. Nitrogen isotherms at the temperature of liquid nitrogen were measured using a Micromeritics ASAP Tristar. The samples were outgassed for 10 h at 150 °C before the measurement. Pore-size distribution for mesopores was calculated using Barrett–Joyner–Halenda (BJH) model. The content of Au was determined from inductively coupled plasma (ICP) with a Perkin-Elmer plasma 40 emission spectrometer. The ^{13}C NMR spectra were recorded on a Bruker Avance-400WB spectrometer using CP-TOSS program with 7.5 mm of MAS probe, 12 kHz of spinning rate, repetition time of 3 s, contact time of 1 s. XPS spectra were performed by a Thermo ESCALAB 250, and the binding energies were calibrated by C1s peak (284.9 eV). IR spectra were recorded using a Bruker 66 V FTIR spectrometer.

2.4. Catalytic tests

Olefin oxidations were carried out in a 40-ml glass reactor with a magnetic stirrer. Typically, substrate, solvent, and catalyst were mixed in the reactor, then the mixture was stirred (900 rpm). After increasing the temperature (the temperature was measured with a thermometer in an oil bath), pure O_2 was introduced and sealed in the reaction system at atmosphere pressure by a U tube made by ourselves. After reaction, the products were analyzed by gas chromatography (GC-14C and GC-17A, Shimadzu, FID) with a flexible quartz capillary column (OV-17 or OV-1). The recyclability of the catalyst was tested by separating it from the reaction system by centrifugation, washing with large quantity of methanol, and drying at 373 K for 6 h, then the catalyst was reused in the next reaction.

2.5. Computational methodology

We performed DFT calculation on a model Au–Py system to better interpret the electronic interaction between the Py terminal

and Au nanoparticles. We use Au_{55} (quasicrystalline I_h structure) with a Py as our model nanoparticle structure to examine the interaction between Py and the Au NP; Au_{55} has been studied both theoretically and experimentally [69–71]. For this investigation, we used the plane-wave computational package VASP [72,73] with ultrasoft pseudopotential and within both the local-density approximation (LDA) and the generalized gradient approximation (GGA PW91). The unit cell was a cube of 20.0 Å, and the plane-wave cutoff and convergence criteria were set automatically to medium precision by keyword (PREC = med), which means that for the Au_{55} nanoparticle E_{cut} = 179.7 eV (E_{aug} = 303.0 eV for the potential) and for Au_{55}–Py E_{cut} = 396.0 eV (E_{aug} = 700.0 eV for the potential as the potentials for hydrogen are very sharp). A convergence criteria of 0.1×10^{-2} eV (0.1×10^{-3} eV) were used for the ionic motion (electronic SCF).

3. Results and discussion

3.1. Characterization of Au catalysts

Fig. 1 shows ^{13}C NMR spectra of SBA-15, SBA-15-N, Au/SBA-15-Py, DETA, and Py species. SBA-15 has not obvious signal associated with carbon species (Fig. 1a), indicating nearly complete removal of the copolymer surfactant. SBA-15-N gives peaks at 11.0, 23.0, 41.1, 49.5, and 58.0 ppm (Fig. 1b), which are well consistent with the signals of DETA species (Fig. 1d). Interestingly, Au/SBA-15-Py exhibits additional peaks at 29.1, 57.1, and 180.0 ppm (Fig. 1c), in nice agreement with the presence of pyrrolidone species (Fig. 1e). The appearance of 165 ppm peak (Fig. 1c) indicates the presence of amide that acts as the linkage of DETA and pyrrolidone species [74]. These results suggest that both DETA and Py species are successfully grated on the surface of mesoporous SBA-15, as proposed in Scheme 1.

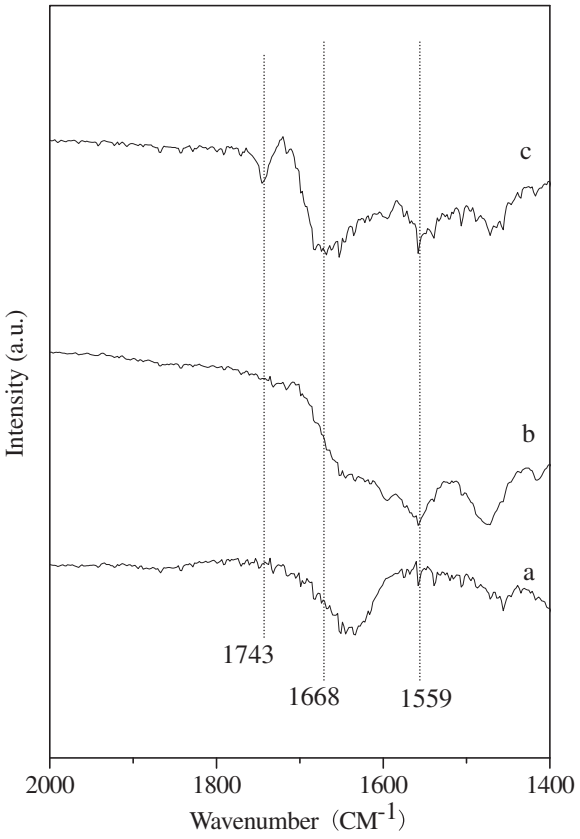

Fig. 2. IR spectra of: (a) SBA-15, (b) SBA-15-N, and (c) Au/SBA-15-Py samples.

Fig. 2 shows IR spectra of SBA-15-N and Au/SBA-15-Py catalysts. The band at 1559 cm^{-1} (Fig. 2b and c) is assigned to C—N bond [75,76]. Particularly, Au/SBA-15-Py has additional bands at 1668 and 1743 cm^{-1}, indicating the presence of C═O bonds attributed to pyrrolidone species in Au/SBA-15-Py [75]. These results are well consistent with successful grafting of DETA and Py species on SBA-15 characterized from ^{13}C NMR spectroscopy.

Fig. 3 shows XRD patterns in small angles of Au/SBA-15-Py and Au/SBA-15-N. Both show three well-resolved XRD peaks in the region of 0.6–2° indexed to (1 1 0), (2 0 0), and (2 1 1) reflections of hexagonal mesoporous arrays, indicating that their hexagonal mesostructure is well remained. In nitrogen isotherms (Fig. 4), both samples exhibit typical type-IV curve, giving a hysteresis loop at relative pressure of 0.52–0.74. Correspondingly, they exhibit pore-size distribution at 6.3–6.9 nm, which is smaller than that (8.4 nm) of SBA-15. In addition, Au/SBA-15-Py and Au/SBA-15-N show relatively low surface area (222 and 286 m^2/g), compared with SBA-15 (948 m^2/g, Table 1). All of these results support that Au nanoparticles and organic species including DETA and Py exist in the mesopores [76].

We have also characterized Au NPs by TEM and wide-angle XRD techniques. TEM images (Fig. 5) give direct observation that Au NPs with similar sizes of 2–3 nm are highly dispersed in the mesopores of both Au/SBA-15-Py and Au/SBA-15-N. Furthermore, the sample wide-angle XRD patterns (Fig. 3) show a very broad diffraction

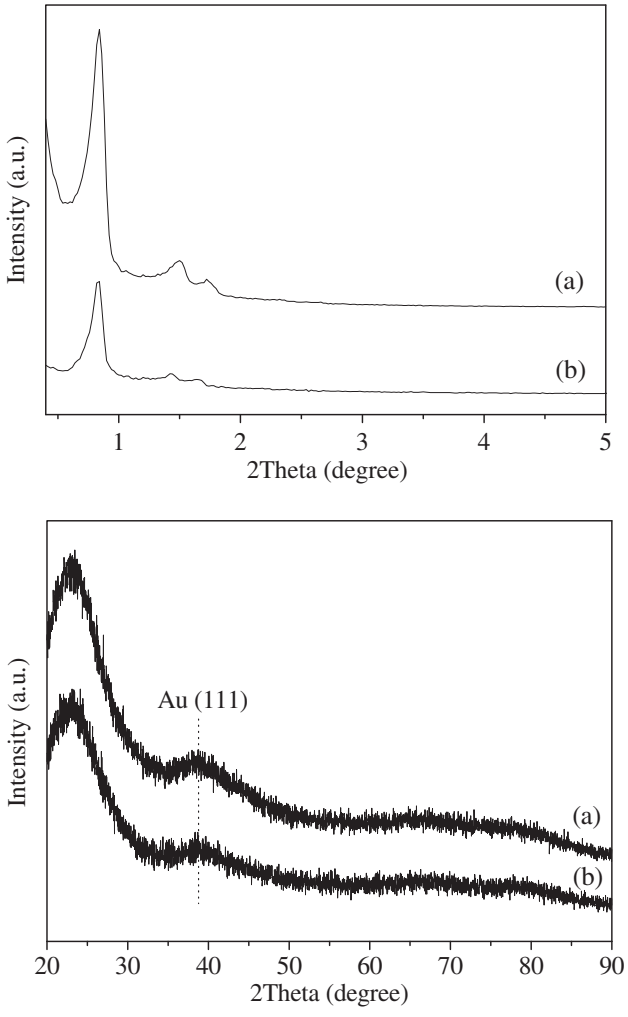

Fig. 3. Small (top) and wide (bottom) angle XRD patterns of: (a) Au/SBA-15-N and (b) Au/SBA-15-Py samples.

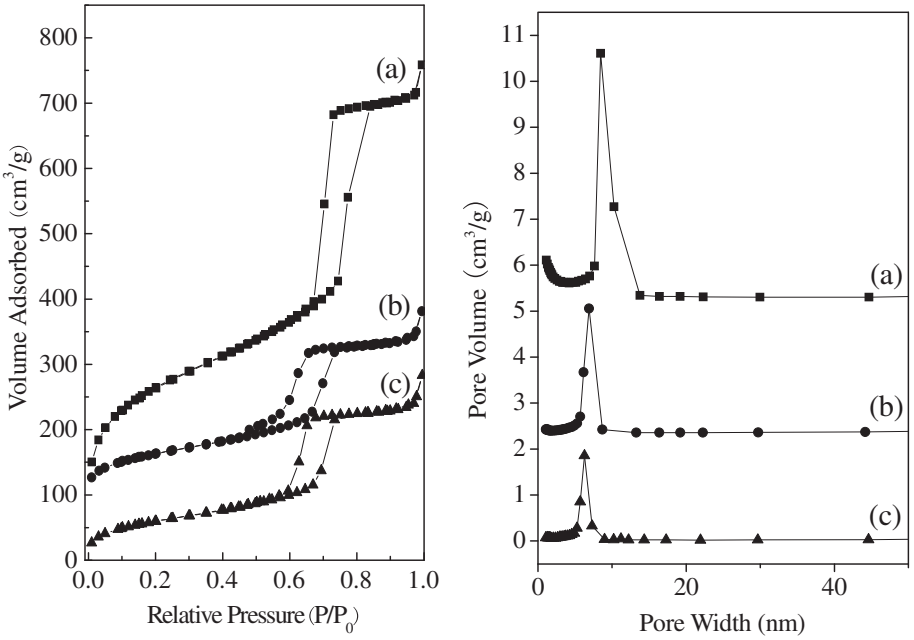

Fig. 4. Nitrogen adsorption–desorption isotherms and pore-size distribution of: (a) SBA-15, (b) Au/SBA-15-N, and (c) Au/SBA-15-Py samples.

Table 1
Textural parameters, Au content, and particle size of SBA-15, Au/SBA-15-N, and Au/SBA-15-Py samples.

Sample	S_{BET} (m^2/g)	Pore width (nm)	Au content (wt.%)	Au nanoparticle size (nm)	
				Scherrer Equation	TEM
SBA-15	948	8.4	–	–	–
Au/SBA-15-N	286	6.9	2.6	2.2	2.0–3.0
Au/SBA-15-Py	222	6.3	2.7	2.1	2.0–3.0

peak at 38.7° associated with (1 1 1) incidence of Au NPs. According to Scherrer equation [77,78], it is estimated that the average sizes of Au NPs in Au/SBA-15-Py and Au/SBA-15-N are close to 2.1 and 2.2 nm (Table 1), confirming similar Au NP size in both catalysts.

Fig. 6 shows Au4f XPS spectra of Au/SBA-15-N and Au/SBA-15-Py samples. Au/SBA-15-N gives the binding energy of $Au4f_{7/2}$ at 84.0 eV, which is typically assigned to the metallic Au [47,79]. Interestingly, Au/SBA-15-Py exhibits $Au4f_{7/2}$ binding energy at 83.4 eV, with 0.6 eV of downshift from Au/SBA-15-N, indicating the presence of an interaction between Au NPs and Py species. Clearly, the downshift of $Au4f_{7/2}$ binding energy suggests that the surface of Au NPs over Au/SBA-15-Py is negatively charged, compared with Au/SBA-15-N [79].

3.2. Catalytic results

Table 2 presents catalytic data in cyclohexene oxidation by molecular oxygen under atmospheric pressure using various solvents over Au/SBA-15-Py and Au/SBA-15-N catalysts. Notably, both catalysts are active, but Au/SBA-15-Py always shows much higher activity than Au/SBA-15-N. For example, in toluene solvent, Au/SBA-15-Py shows conversion at 54.0% (Table 2, entry 1), while Au/SBA-15-N gives low activity (31.2%, Table 2, entry 2); in 1,4-dimethylbenzene solvent, Au/SBA-15-Py shows conversion at 18.7% (Table 2, entry 5), which is much higher than that (5.3%, Table 2, entry 6) of Au/SBA-15-N. In addition, it is also observed that the solvent strongly influences the catalytic activity (Table 2), which might be associated with their distinguishable polarity. Notably, in 1,4-dimethylbenzene solvent, the addition of TBHP as radical initiator is necessary. If TBHP is absent, the Au catalysts are almost inactive. Similar phenomena have been reported previously [4,80].

In cyclohexene oxidation, the major products are cyclohexene epoxide, 2-cyclohexen-1-ol, 2-cyclohexen-1-one, and 1,2-cyclohexanedione. The by-products include CO_2 and the products less than C_6 [4]. To understand the reaction route, various products were used as starting reactants to perform oxidations (Table 3). When cyclohexene epoxide was used as a substrate, Au/SBA-15-Py was inactive (Table 3, entry 1), which indicates that the products of 2-cyclohexen-1-ol, 2-cyclohexen-1-one, and 1,2-cyclohexanedione are from direct oxidation of cyclohexene, rather than transformation from cyclohexene epoxide intermediate. When 2-cyclohexen-1-one or 1,2-cyclohexanedione were used as a substrate, Au/SBA-15-Py was still inactive (Table 3, entry 2 and 3), which suggests that the formation of by-products is not from over-oxidation or decomposition of these compounds. When 2-cyclohexen-1-ol was used as a substrate, 2-cyclohexen-1-one was selectively formed (Table 3, entry 4). All of these results suggest that by-products in cyclohexene oxidation are formed from direct over-oxidation of cyclohexene, and the products of cyclohexene oxide, 2-cyclohexen-1-ol, and 1,2-cyclohexanedione are resulted from direct oxidation of cyclohexene (Scheme 2).

Furthermore, the Au/SBA-15-Py catalyst was treated in toluene at 100 °C for 8 h. After filtration of Au/SBA-15-Py catalyst, the solution was used as new catalyst for cyclohexene oxidation. As a result, no products were found. Additionally, the concentration of Au in the treated solution was less than 0.01 ppm (ICP analysis). These results indicate that no Au leaching occurs at Au/SBA-15-Py catalyst in cyclohexene oxidation.

Moreover, Au/SBA-15-Py catalyst has excellent recyclability in cyclohexene oxidation (Fig. 7a). For example, after reuse, there is no loss for catalytic activity (54%); after recycles for four times, Au/SBA-15-Py catalyst still shows the conversion at 51%, indicating its excellent recyclability. Notably, $Au4f_{7/2}$ XPS spectrum of Au/SBA-

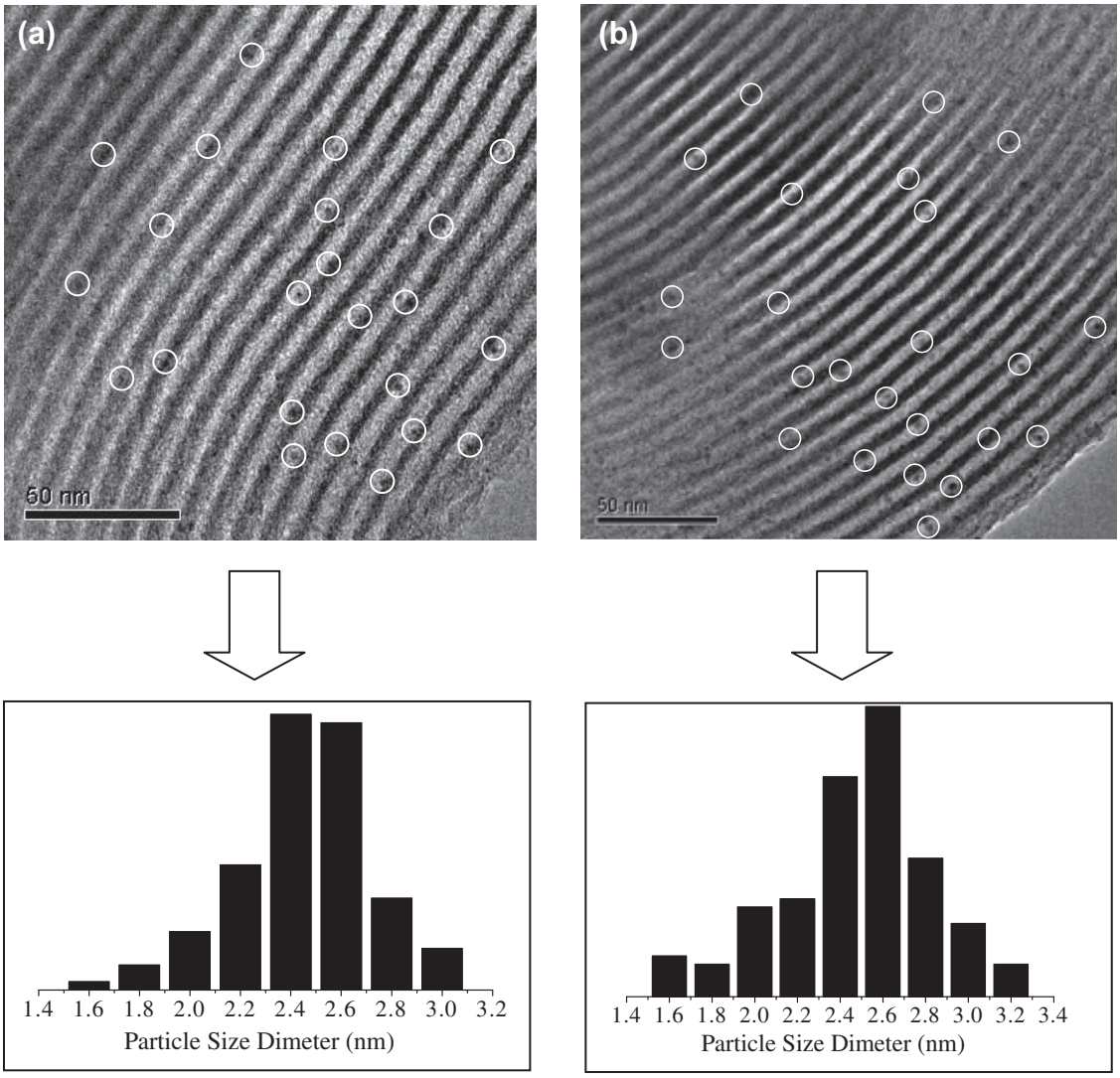

Fig. 5. TEM images (top) and Au nanoparticle size distribution (bottom) of: (a) Au/SBA-15-Py and (b) Au/SBA-15-N samples (The scale bars are both 50 nm).

15-Py recycled for four times shows very similar binding energy (83.5 eV) to that (83.4 eV) of the fresh catalyst, supporting that Au/SBA-15-Py has good stability during cyclohexene oxidation.

Fig. 8 shows dependences of activities on reaction time at low conversion (less than 5%) in cyclohexene oxidation at the temperature of 373–393 K over Au/SBA-15-Py and Au/SBA-15-N catalysts. After fitting, we can estimate initial reaction rate (r_0). According to Arrhenius equation, activation energies (E_a) of Au/SBA-15-Py and Au/SBA-15-N catalysts were calculated (Fig. 9), yielding 22.0 and 35.1 kJ/mol, respectively. These results confirm that oxidation of cyclohexene over Au/SBA-15-Py is much easier than that over Au/SBA-15-N catalyst.

It is worth mentioning that Au/SBA-15-Py catalyst is very active in cyclohexene oxidation under solvent-free condition (Table 4). Au/SBA-15-Py can give a turnover frequency (TOF) of 12,000 h^{-1} (Table 4, entry 1), which is extremely high for the oxidation of olefins on Au catalysts [11]. In contrast, Au/SBA-15-N gives a TOF at 6400 h^{-1} (Table 4, entry 2), other Au catalysts including Au/TiO_2, Au/MgO and Au/SiO_2 also show relatively low TOF (7020, 4009, and 4712 h^{-1}, Table 4, entry 3–5). These results suggest the high activity of Au sites on Au/SBA-15-Py in solvent-free cyclohexene oxidation.

Table 5 presents catalytic data in styrene oxidation by molecular oxygen under atmospheric pressure using various solvents over Au/SBA-15-Py and Au/SBA-15-N catalysts. Generally, styrene is not easy to be oxidized using molecular oxygen on Au catalysts [11,81]. As same as cyclohexene oxidation, Au/SBA-15-Py in styrene oxidation still gives much higher activity than Au/SBA-15-N. For example, in toluene solvent, Au/SBA-15-Py exhibits the conversion at 37.4% (Table 5, entry 1), while Au/SBA-15-N gives the conversion at 15.6% (Table 5, entry 2); in MeCN solvent, Au/SBA-15-Py and Au/SBA-15-N show the conversion at 22.0% and 11.0%, respectively (Table 5, entry 3 and 4).

Notably, the use of solvent in styrene oxidation not only influences the activity but also changes the product selectivity. For example, in toluene solvent, the selectivity for styrene epoxide is only 3–4% (Table 5, entry 1 and 2). However, when 1,4-dimethylbenzene solvent was used, the selectivity for styrene epoxide reaches to 10–14% (Table 5, entry 5 and 6). This phenomenon might be related to that the formation of C—O—C bonds is favorable in the presence of non-polar solvent [4].

Fig. 7b shows the recyclability of Au/SBA-15-Py in styrene oxidation. After recycles for four times, the catalyst still remains its activity, indicating its excellent recyclability.

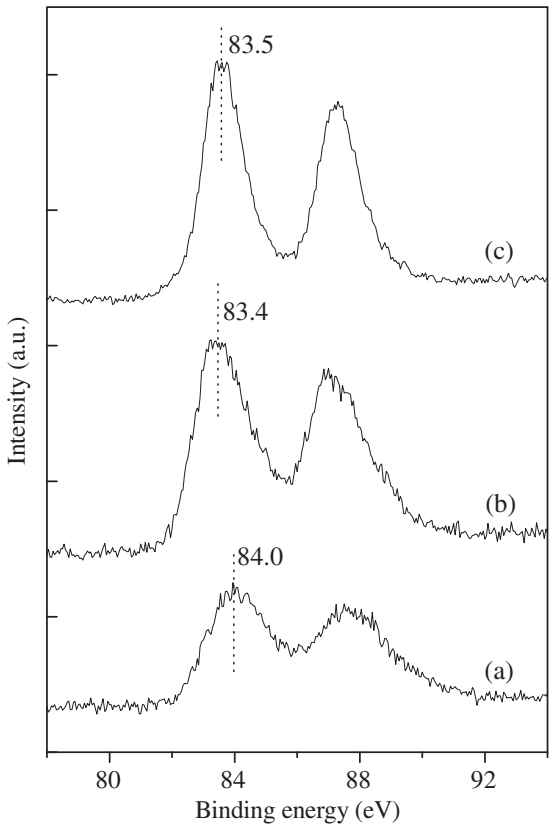

Fig. 6. Au4f XPS spectra of: (a) Au/SBA-15-N, (b) Au/SBA-15-Py, and (c) Au/SBA-15-Py recycled for four times.

Table 3
Catalytic activities in oxidations of various substrates.[a]

Entry	Substrate	Conversion (%)	Selectivity (%)
1	Cyclohexene epoxide	<1	–
2	2-Cyclohexen-1-one	<1	–
3	1,2-Cyclohexanedione	<1	–
4	2-Cyclohexen-1-ol	26.0	>99.5[b]

[a] Reaction conditions 6 mmol of substrate, 10 ml of toluene solvent, 80 mg of Au/SBA-15-Py catalyst, time for 8 h, temperature of oil bath at 373 K.
[b] Selectivity for 2-cyclohexen-1-one.

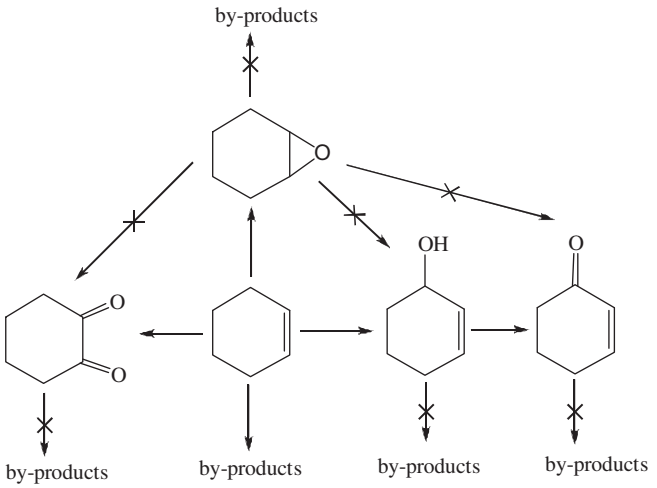

Scheme 2. Proposed routes for the formation of products and by-products in cyclohexene oxidation.

3.3. DFT calculations

We carried out DFT (both LDA and GGA) calculations on two model systems of an isolated Au_{55} nanoparticle and an Au_{55} NP with one Py molecule attached (Fig. 10a). The results from both LDA and GGA are very similar; for clarity, we only present the LDA results here. The partial density of electronic states (DOS) for the Au_{55}, Py, and Au_{55}-Py are shown in Fig. 10b. From the DOS, We find that the electronic properties of Py molecule present obvious differences after the molecule is attached on the Au_{55} nanoparticle. The frontier orbitals of the Py molecule, which is largely a contribution from the oxygen atom, have a strong overlap with the frontier states of an Au atom on the NP surface.

Previously, it was reported that Au_{55} NPs show strong oxidation resistance due to the unique geometry and the electronic structure [11]. In this work, we find that the DOS plot (Fig. 10b) of the isolated Au_{55} has a small energy gap, which is not promising in oxidation reactions. However, the DOS of the Py molecule attached on

Table 2
Catalytic data in cyclohexene oxidation by molecular oxygen over Au/SBA-15-Py and Au/SBA-15-N catalysts.[a]

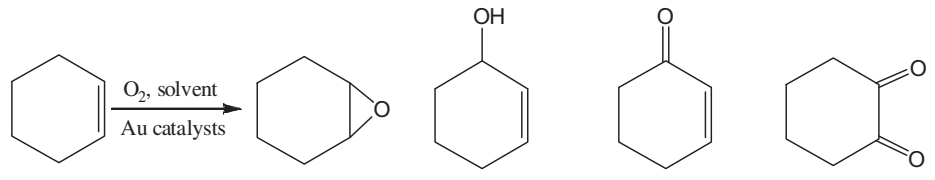

cyclohexene | cyclohexene epoxide **1** | 2-cyclohexen-1-ol **2** | 2-cyclohexen-1-one **3** | 1,2-cyclohexanedione **4**

Entry	Solvent	Catalyst	Conversion (%)	Product selectivity[b] (%)				
				P1	P2	P3	P4	P5
1	Toluene	Au/SBA-15-Py	54.0	7	21	36	3	33
2	Toluene	Au/SBA-15-N	31.2	3	33	44	1	19
3	MeCN	Au/SBA-15-Py	40.2	4	16	38	7	35
4	MeCN	Au/SBA-15-N	32.9	9	19	35	11	26
5	1.4-Dimethylbenzene[c]	Au/SBA-15-Py	18.7	1	7	35	44	14
6	1.4-Dimethylbenzene[c]	Au/SBA-15-N	5.3	2	11	21	50	18

[a] 6 mmol of cyclohexene, 10 ml of solvent, 80 mg of catalyst, time for 8 h, temperature of oil bath at 373 K.
[b] P1, cyclohexene epoxide; P2, 2-cyclohexen-1-ol; P3, 2-cyclohexen-1-one; P4, 1,2-cyclohexanedione; P5, CO_2 and other organic products with less than six C atoms.
[c] *t*-butyl hydroperoxide (TBHP, 3 mol% based on substrate) is added. The conversion of cyclohexene is very low (<1%) without TBHP in 1,4-dimethylbenzene solvent.

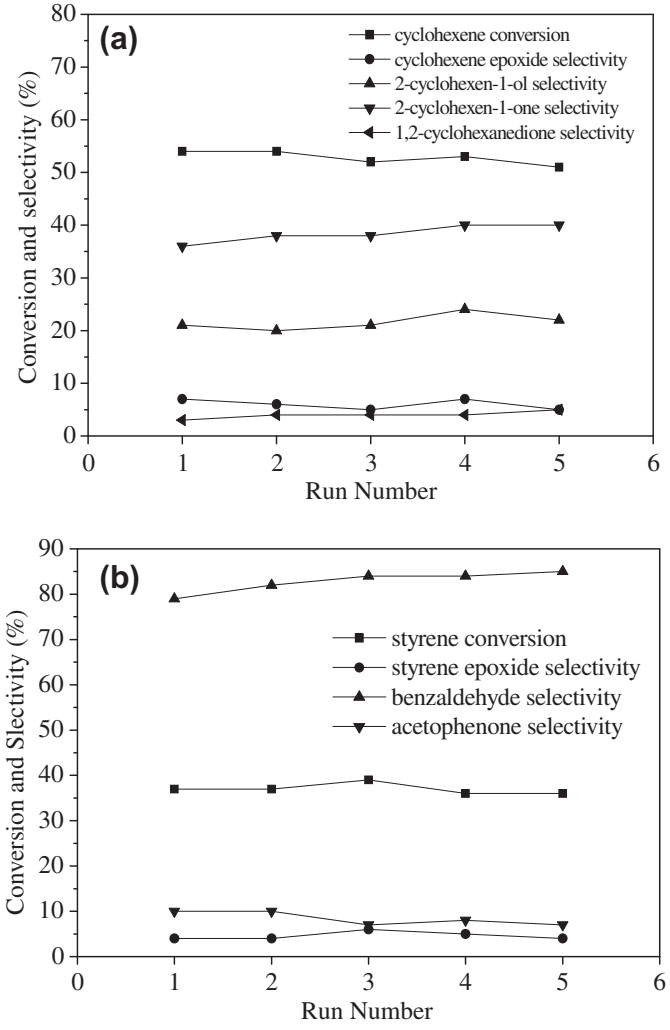

Fig. 7. Recyclable data in: (a) cyclohexene and (b) styrene oxidations over Au/SBA-15-Py catalyst.

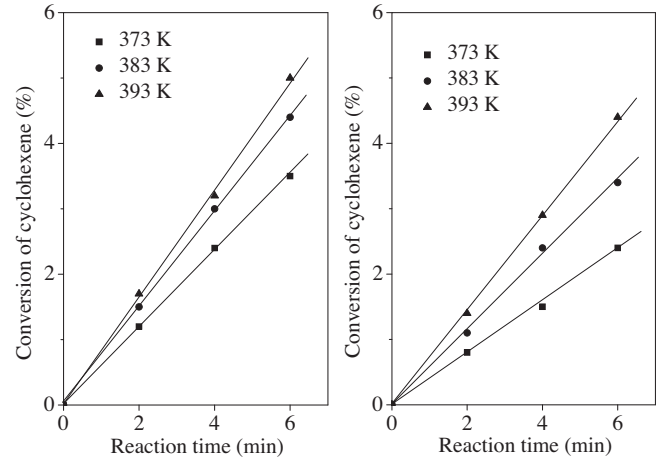

Fig. 8. Dependences of activities on reaction time at low conversion in cyclohexene oxidation at the temperature of 373–393 K over Au/SBA-15-Py and Au/SBA-15-N catalysts.

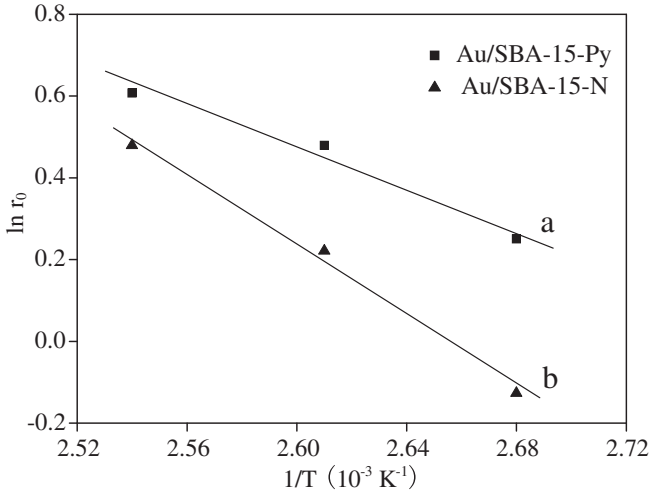

Fig. 9. Experimental points correlating the inverse of the absolute temperature (1/*T*) with the initial reaction rates (ln r_0) with catalysts of Au/SBA-15-Py and Au/SBA-15-N. Two straight lines are made with the best fitting of the experimental points.

Table 4
Solvent-free oxidation of cyclohexene by molecular at atmospheric pressure over Au/SBA-15-Py catalyst.[a].

Entry	Catalyst	TOF (h^{-1})
1	Au/SBA-15-Py	12,000
2	Au/SBA-15-N	6400
3	Au/TiO_2	7020
4	Au/MgO	4009
5	Au/SiO_2	4712

[a] Reaction conditions: 100 mmol of cyclohexene, 15 mg of catalyst, TBHP (3 mol% based on cyclohexene), O_2 at atmospheric pressure, temperature of oil bath at 413 K, reaction time for 20 min.

Table 5
Catalytic data in styrene oxidation by molecular oxygen over Au/SBA-15-Py and Au/SBA-15-N catalysts.[a]

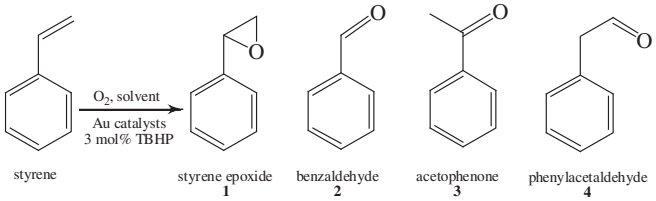

Entry	Solvent	Catalyst	Conversion (%)	Product selectivity[b] (%)				
				P1	P2	P3	P4	P5
1	Toluene	Au/SBA-15-Py	37.4	4	79	10	–	7
2	Toluene	Au/SBA-15-N	15.6	3	86	6	1	4
3	MeCN	Au/SBA-15-Py	22.0	3	45	2	–	50
4	MeCN	Au/SBA-15-N	11.0	5	52	–	–	43
5	1.4-Dimethylbenzene	Au/SBA-15-Py	30.2	14	32	26	–	30
6	1.4-Dimethylbenzene	Au/SBA-15-N	17.3	10	40	16	4	30

[a] 6 mmol of styrene, 10 ml of solvent, 80 mg of catalyst, time for 8 h, temperature of oil bath at 373 K; *t*-butyl hydroperoxide (TBHP, 3 mol% based on substrate) is added.

[b] P1, styrene epoxide; P2, benzaldehyde; P3, acetophenone; P4, phenylacetaldehyde; P5, phenylacetic acid, benzoic acid, ester, and some others.

the Au_{55} NP present quite a different DOS before (Fig. 10c) and after (Fig. 10d) the attachment of Py on the Au_{55} nanoparticle. The *discrete* molecule orbitals induce specific electronic modification to the Au_{55} NP; therefore, the delocalized electrons distributed onto the Au NP surface changes after the Py attachment. Because there is only one Py molecule attached Au_{55} model, we speculate

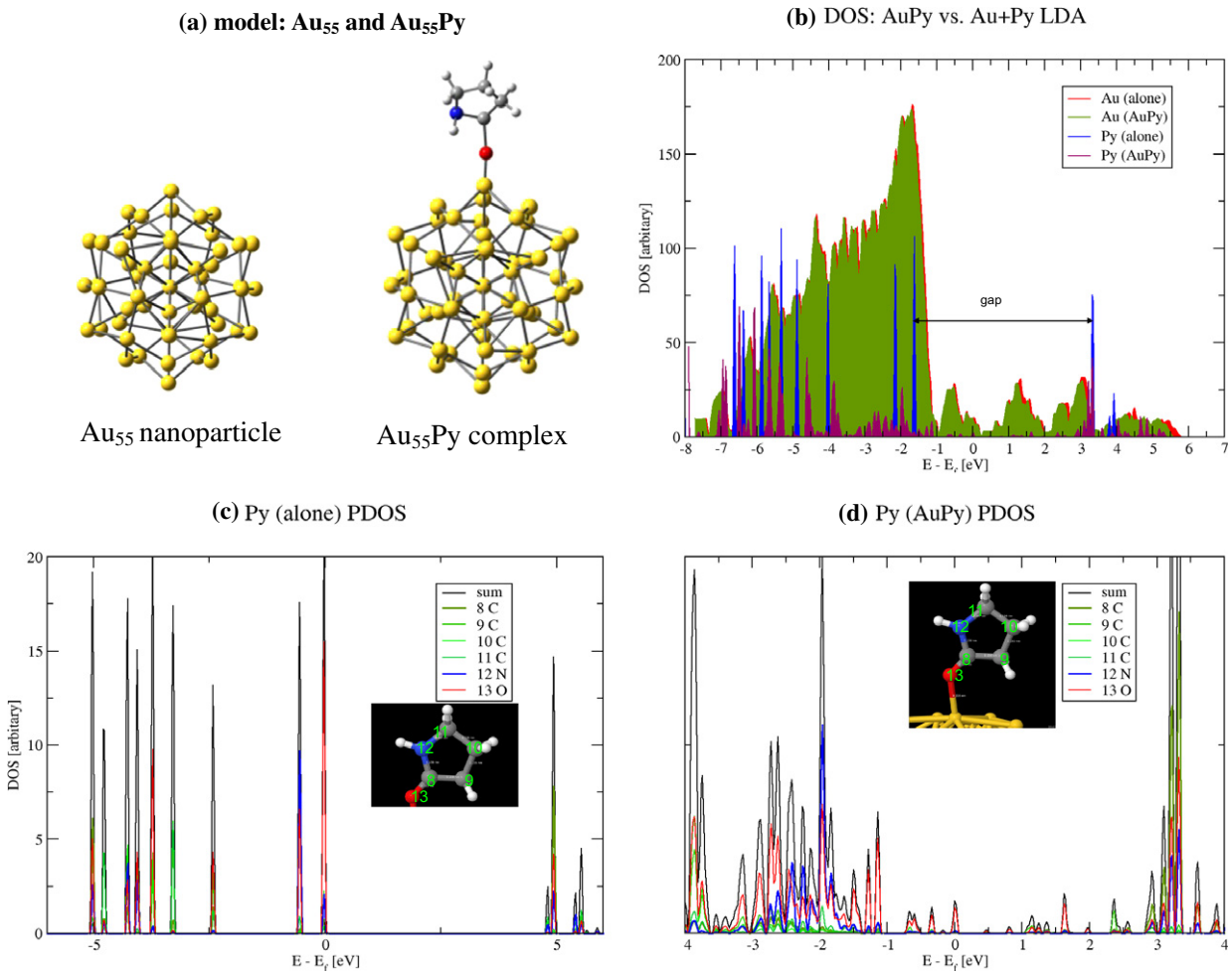

Fig. 10. (a) Structures of Au_{55} nanoparticle and $Au_{55}Py$ complex; (b) The density of states (DOS) of Py alone, Py of $Au_{55}Py$, Au_{55} alone, and Au_{55} after Py attached, the gap showing in the plots is the HOMO–LUMO gap of Py molecule alone; the projected density of states (PDOS) of (c) all the atoms of Py molecule itself and (d) Py molecule on Au_{55} nanoparticle.

that more Py attached will serve as a functional group on the NP surfaces and induce more electronic modification of the entire Au nanoparticle. This modification induces imbalanced localization of charge distribution on the entire Au nanoparticle, which will cause more negative charge on the Au NP surface and assist oxidation reaction occurring. In accordance with the XPS results shown in Fig. 6, we propose that the Py attachment on Au NP induces charge redistribution on the surface of the Au NP; therefore, the catalytic activity is accordingly enhanced.

4. Conclusions

We find that Au nanoparticles are highly dispersed in the mesopores of pyrrolidone-modified SBA-15 (Au/SBA-15-Py). These ligand-modified Au nanoparticles are highly efficient and stable heterogeneous catalysts for oxidations of cyclohexene and styrene by molecular oxygen at atmospheric pressure. The superior catalytic properties over Au/SBA-15-Py are related to the interaction between pyrrolidone species and Au nanoparticles, in strong agreement with present density-functional theory calculations included in this work.

Acknowledgments

This work is supported by the National Natural Science Foundation of China (20973079) and the State Basic Research Project of China (2009CB623501). Dr. H. Wang was supported in part by the (USA) National Science Foundation (DMR-0903225) and by the Advanced Energy Initiative of West Virginia University. P. Hapala was supported by the Czech Republic Grant No. SVV-2010-263303.

References

[1] G.A. Barf, R.A. Sheldon, J. Mol. Catal. A 102 (1995) 23.
[2] B. Notari, Stud. Surf. Sci. Catal. 60 (1991) 343.
[3] J.R. Monnier, Appl. Catal. A 221 (2001) 73.
[4] M.D. Hughes, Y.-J. Xu, P. Jenkins, P. McMorn, P. Landon, D.I. Enache, A.F. Carley, G.A. Attard, G.J. Hutchings, F. King, E.H. Stitt, P. Johnston, K. Griffin, C.J. Kiely, Nature 437 (2005) 1132.
[5] G. Cainelli, G. Cardillo, Chromium Oxidations in Organic Chemistry, Springer, Berlin, 1984.
[6] B. Hinzen, S.V. Ley, J. Chem. Soc., Perkin Trans. 1 (1997) 1907.
[7] N.S. Patil, B.S. Uphade, P. Jana, S.K. Bharagava, V.R. Choudhary, J. Catal. 223 (2004) 236.
[8] Y. Liu, H . Tsunoyama, T. Akita, T. Tsukuda, Chem. Commun. 46 (2010) 550.
[9] G.-J. ten Brink, I.W.C.E. Arends, R.A. Sheldon, Science 287 (2000) 1636.
[10] X. Meng, K. Lin, X. Yang, Z. Sun, D. Jiang, F. -S. Xiao, J. Catal. 218 (2003) 460.
[11] M. Turner, V.B. Golovko, O.P.H. Vaughan, P. Abdulkin, A. Berenguer-Murcia, M.S. Tikhov, B.F.G. Johnson, R.M. Lambert, Nature 454 (2008) 981.
[12] Y.H. Lin, I.D. Williams, P. Li, Appl. Catal. A 150 (1997) 221.
[13] S. Rayati, M. Koliaei, F. Ashouri, S. Mohebbi, A. Wojtczak, A. Kozakiewicz, Appl. Catal. A 346 (2008) 65.
[14] S.K. Ginotra, V.K. Singh, Tetrahedron 62 (2006) 3573.
[15] P.P. Knopsgerrits, D. Devos, F. Thibaultstarzyk, P.A. Jacobs, Nature 369 (1994) 543.
[16] T. Hayashi, K. Tanaka, M. Haruta, J. Catal. 178 (2008) 566.
[17] G.J. Hutchings, Catal. Today 122 (2007) 196.

[18] L. Kesavan, R. Tiruvalam, M.H.A. Rahim, M.I. ban Saiman, D.I. Enache, R.L. Jenkins, N. Dimitratos, J.A. Lopes-Sanchez, S.H. Taylor, D.W. Knight, C.J. Kiely, G.J. Hutchings, Science 331 (2011) 195.
[19] G.J. Hutchings, J. Catal. 96 (1985) 292.
[20] M. Haruta, T. Koboyashi, H. Sano, N. Yamada, Catal. Lett. 16 (1987) 405.
[21] A.A. Herzing, C.J. Kiely, A.F. Carley, P. Landon, G.J. Hutchings, Science 321 (2008) 1331.
[22] T.V. Choudhary, D.W. Goodman, Top. Catal. 21 (2002) 25.
[23] C.W. Corti, R.J. Holliday, D.T. Thompson, Appl. Catal. A 291 (2005) 253.
[24] G.J. Hutchings, M.S. Hall, A.F. Carley, P. Landon, B.E. Solsona, C.J. Kiely, A. Herzing, M. Makkee, J.A. Moulijn, A. Overweg, J.C. Fierro-Gonzalez, J. Guzman, B.C. Gates, J. Catal. 242 (2006) 71.
[25] A. Corma, H. Garcia, Chem. Soc. Rev. 37 (2008) 2096.
[26] A. Grirrane, A. Corma, H. Garcia, J. Catal. 268 (2009) 350.
[27] A. Corma, I. Dominguez, A. Domenech, V. Fornes, C.J. Gomez-Garcia, T. Rodenas, M.J. Sabater, J. Catal. 265 (2009) 238.
[28] A.S.K. Hashmi, G.J. Hutchings, Angew. Chem. Int. Ed. 45 (2006) 7896.
[29] A. Abad, P. Concepcion, A. Corma, H. Garcia, Angew. Chem. Int. Ed. 44 (2005) 4066.
[30] J.C.F. Gonzales, B.C. Gates, Chem. Soc. Rev. 37 (2008) 2127.
[31] V.A. Guerrero, B.C. Gates, Chem. Commun. (2007) 3210.
[32] J. Guzman, B.C. Gates, J. Am. Chem. Soc. 126 (2004) 2672.
[33] Y. Hao, M. Mihaylov, E. Ivanova, K. Hadjiivanov, H. Knozinger, B.C. Gates, J. Catal. 261 (2009) 137.
[34] C. Raptis, H. Garcia, M. Stratakis, Angew. Chem. Int. Ed. 48 (2009) 3133.
[35] L.F. Chen, J.C. Hu, R. Richards, J. Am. Chem. Soc. 131 (2009) 914.
[36] X. Zhang, H. Shi, B.-Q. Xu, Angew. Chem. Int. Eds. 44 (2005) 7132.
[37] X. Zhang, H. Shi, B.-Q. Xu, Catal. Today 122 (2007) 330.
[38] R. Zhao, D. Ji, G.M. Lv, G. Qian, L. Yan, X.L. Wang, J.S. Suo, Chem. Commun. (2004) 904.
[39] G.M. Lu, D. Ji, G. Qian, Y.X. Qi, X.L. Wang, J.S. Suo, Appl. Catal. A 280 (2005) 175.
[40] W. Yan, S. Brown, Z. Pan, S.M. Mahurin, S.H. Overbury, S. Dai, Angew. Chem. Int. Ed. 45 (2006) 3614.
[41] W. Yan, S.M. Mahurin, Z. Pan, S.H. Overbury, S. Dai, J. Am. Chem. Soc. 127 (2005) 10480.
[42] Y. Zhen, S. Chinta, A.A. Mohamed, J.P. Fackler, D.W. Goodman, J. Am. Chem. Soc. 127 (2005) 1604.
[43] B.N. Zope, D.D. Hibbitts, M. Neurock, R.J. Davis, Science 330 (2010) 74.
[44] M.S. Chen, D. Kumar, C.W. Yi, D.W. Goodman, Science 310 (2005) 291.
[45] B.P.C. Hereijgers, B.M. Weckhuysen, J. Catal. 270 (2010) 16.
[46] X.Y. Deng, B.K. Min, A. Guloy, C.M. Friend, J. Am. Chem. Soc. 127 (2005) 9267.
[47] R. Si, M. Flyzani-Stephanopoulos, Angew. Chem. Int. Ed. 47 (2008) 2884.
[48] F.-Z. Su, Y.-M. Liu, L.-C. Wang, Y. Cao, H.-Y. He, K.-N. Fan, Angew. Chem. Int. Ed. 47 (2008) 334.
[49] H. Sun, F. -Z Su, J. Ni, Y. Cao, H.-Y. He, K.-N. Fan, Angew. Chem. Int. Ed. 48 (2009) 4390.
[50] C.-M. Wang, K.-N. Fan, Z.-P. Liu, J. Catal. 266 (2009) 343.
[51] W.B. Hou, N.A. Dehm, R.W.J. Scott, J. Catal. 253 (2008) 22.
[52] X.S. Tian, W.P. Deng, M. Liu, Q.H. Zhang, Y. Wang, Chem. Commun. 46 (2009) 7179.
[53] W.H. Fang, Q.H. Zhang, J. Chen, W.P. Deng, Y. Wang, Chem. Commun. 46 (2010) 1547.
[54] C.T. Campbell, Science 306 (2004) 234.
[55] K.N. Heck, M.O. Nutt, P. Alvarez, M.S. Wong, J. Catal. 267 (2009) 97.
[56] B. Jorgensen, S.E. Christiansen, M.L.D. Thomsen, C.H. Christiansen, J. Catal. 251 (2007) 332.
[57] J. Han, Y. Liu, R. Guo, J. Am. Chem. Soc. 131 (2009) 2060.
[58] T. Mitsudome, A. Noujima, T. Mizugaki, K. Jitsukawa, K. Kaneda, Green Chem. 11 (2009) 793.
[59] T. Mitsudome, A. Noujima, T. Mizugaki, K. Jitsukawa, K. Kaneda, Adv. Synth. Catal. 351 (2009) 1890.
[60] C.Y. Ma, Z. Mu, J.J. Li, Y.G. Jin, J. Cheng, G.Q. Lu, Z.P. Hao, S.Z. Qiao, J. Am. Chem. Soc. 132 (2010) 2608.
[61] C.Y. Ma, B.J. Dou, J.J. Li, J. Cheng, Q. Hu, Z.P. Hao, S.Z. Qiao, Appl. Catal. B 92 (2009) 202.
[62] D.S. Wang, Y.D. Li, J. Am. Chem. Soc. 132 (2010) 6280.
[63] J.F. Liu, W. Chen, X.W. Liu, K.B. Zhou, Y.D. Li, Nano Res. 1 (2008) 46.
[64] Y.H. Deng, Y. Cai, Z.K. Sun, J. Liu, C. Liu, J. Wei, W. Li, C. Liu, Y. Wang, D.Y. Zhao, J. Am. Chem. Soc. 132 (2010) 8466.
[65] H. Tsunoyama, H. Sakurai, Y. Negishi, T. Tsukuda, J. Am. Chem. Soc. 127 (2005) 9374.
[66] H. Tsunoyama, N. Ichikuni, H. Sakurai, T. Tsukuda, J. Am. Chem. Soc. 131 (2009) 7086.
[67] L. Wang, X.J. Meng, B. Wang, W.Y. Chi, F.-S. Xiao, Chem. Commun. 46 (2010) 5003.
[68] D. Zhao, J. Feng, Q. Huo, N. Melosh, G.H. Fredrickson, B.F. Chmelka, G.D. Stucky, Science 279 (1998) 548.
[69] R.J.C. Batista, M.B.C. Mazzoni, H. Chacham, Nanotechnology 21 (2010) 065705.
[70] A. Vargas, G. Santarossa, M. Iannuzzi, A. Baiker, Phys. Rev. B 80 (2009) 195421.
[71] I.L. Garzon, K. Michaelian, M.R. Beltran, A.P. Amarillas, P. Ordejon, E. Artacho, D.S. Portal, J.M. Soler, Phys. Rev. Lett. 81 (1998) 1600.
[72] G. Kresse, J. Furthmuller, Comput. Mater. Sci. 6 (1996) 15.
[73] G. Kresse, J. Furthmuller, Phys. Rev. B 54 (1996) 11169.
[74] J.A. Hirsch, J. Org. Chem. 44 (1979) 3225.
[75] R.S. Clegg, S.M. Reed, R.K. Smith, B.L. Barron, J.A. Rear, J.E. Hutchison, Langmuir 15 (1999) 8876.
[76] Y. Jin, P. Wang, D. Yin, J. Liu, H. Qiu, N. Yu, Micropor. Mesopor. Mater. 111 (2008) 569.
[77] B. Lee, Z. Ma, Z. Zhang, C. Park, S. Dai, Micropor. Mesopor. Mater. 122 (2009) 160.
[78] E. Sacaliuc, A.M. Beale, B.M. Weckhuysen, T.A. Nijhuis, J. Catal. 248 (2007) 235.
[79] Y.-F. Han, Z. Zhong, K. Ramesh, F. Chen, L. Chen, J. Phys. Chem. C 111 (2007) 3163.
[80] M. Alvaro, C. Aprile, A. Corma, B. Ferrer, H. Garcia, J. Catal. 245 (2007) 249.
[81] X.Y. Deng, C.M. Friend, J. Am. Chem. Soc. 127 (2005) 17178.